are listed in Ref. 5. The right-half of the laminate is discretized by 1152 4CST (constant strain triangle) elements with 2393 node points as a finite element model. Sufficiently finer meshes are used in the vicinity of the hole. Uniform traction forces along the lower edge of the plate are linearly increased up to the maximum average stress $\bar{\sigma}_x = 75$ MPa for 30 s. The interval of the time steps is 0.25 s, and the number of subdivisions that are required for the numerical integration of viscoplastic rate equations is 200 within each global time step. Also, the error tolerance for convergence checking is fixed at 0.02%.

To view the propagation of inelastic deformation in laminates, maps of viscoplastic strain are drawn in Fig. 1b. One of the tensor invariants is selected as a measure of viscoplastic deformation. The plastic deformation spreads near the upper hole boundary in the initial stage because the contact force is largest at that region. At the subsequent time events, the portions that experience the inelastic deformation are gradually widened in all plies. The values of the plastic strain remain high on the hole boundaries in the $\theta = 0$ and 75 directions. Based on this information, it can be considered that the bearing mode will dominate the failure mechanisms of this composite structure with increased load conditions.

Distributions of the normal tractions in the radial and tangential directions are plotted in Fig. 2. The graph of the contact traction $\bar{\sigma}_n$ shows that the contact area varies slightly, about $\theta = 82$ deg when contact clearance is zero. Also the $\bar{\sigma}_\theta$ variations of the viscoplastic analysis deviate from the elastic solutions in $\theta = 0 \sim 15$ range. Figure 3 plots the variations of total strains. The differences between the elastic and elastoviscoplastic solutions are large at $\theta = 0$ and 75 deg, which illustrates that plastic flow in some part of the composite will produce more intense deformations of the structure.

Conclusions

An unmixing–mixing scheme is applied to describe the macroscopic viscoplastic behavior of composite materials. In computational aspects, the penalty finite element methods have provided convenient analysis capabilites for the elastoviscoplastic response of composite structures with complex geometry and boundary condition. The pin-jointed composite plate is solved as a numerical example to illustrate the basic characteristics of the proposed constitutive theory and the analysis capabilities of the numerical methods. The results have shown the propagations of inelastic deformation, the stress distributions in the plies, and the effects of viscoplastic phenomena that are different from the pure elastic cases. Research work, in which a failure criterion consistent with the unmixing–mixing scheme is included for finite element analysis, is in progress and will be reported on in a subsequent paper.

References

[1]Robinson, D. N., and Duffy, S. F., "Continuum Deformation Theory for High-Temperature Metallic Composites," *Journal of Engineering Mechanics*, Vol. 116, No. 4, 1990, pp. 832–844.

[2]Yoon, K. J., and Sun, C. T., "Characterization of Elastic-Viscoplastic Properties of an AS4/ PEEK Thermoplastic Compsite," *Journal of Composite Materials*, Vol. 25, 1991, pp. 1277–1296.

[3]Saleeb, A. F., and Wilt, T. E., "Analysis of the Anisotropic Viscoplastic-Damage Response of Composite Laminates—Continuum Basis and Computational Algorithms," *International Journal for Numerical Methods in Engineering*, Vol. 36, 1993, pp. 1629–1660.

[4]Dvorak, G. J., and Bahei-El-Din, Y. A., "Plasticity Analysis of Fibrous Composites," *Journal of Applied Mechnics*, Vol. 49, 1982, pp. 327–335.

[5]Kim, S. J., and Cho, J. Y., "Role of Matrix in Viscoplastic Behavior of Thermoplastic Composites at Elevated Temperature," *AIAA Journal*, Vol. 30, No. 10, 1992, pp. 2571–2573.

[6]Kim, S. J., and Oden, J. T., "Finite Element Analysis of a Class of Problems in Finite Elastoplasticity Based on the Thermodynamical Theory of Materials of Type N," *Computer Methods in Applied Mechanics and Engineering*, Vol. 53, 1985, pp. 277–302.

[7]Oden, J. T., and Kikuchi, N., "Finite Element Methods for Constrained Problems in Elasticity," *International Journal for Numerical Methods in Engineering*, Vol. 18, 1982, pp. 701–725.

[8]Chang, T. Y., Chen, J. Y., and Chu, S. C., "Viscoplastic Finite Element Analysis by Automatic Subincrementing Technique," *Journal of Engineering Mechanics*, Vol. 114, 1988, pp. 80–96.

Supersonic Flutter Analysis of Stiffened Isotropic and Anisotropic Panels

Dong-Min Lee* and In Lee†
Korea Advanced Institute of Science and Technology, Taejon 305-701, Republic of Korea

I. Introduction

PANEL flutter is a self-excited oscillating phenomenon and involves interactions among elastic, inertia, and aerodynamic forces. Many researchers have studied panel flutter problems for isotropic and anisotropic panels. Dowell[1] gave a comprehensive overview of panel flutter. Applications of the finite element method to linear flutter problems for isotropic panels have been presented by many investigators.[2,3] Recently, for high-performance and advanced aerospace structures, the use of laminated structural components has considerably increased. Hence, various studies[3–6] have been performed for supersonic flutter analysis of anisotropic panels by considering the effects of panel geometry, boundary conditions, lamination scheme, flow directions, and thermal effects.

Also for high-performance applications, the weight saving is an important consideration. It is often necessary to minimize the maximum deflection of skin panel without introducing any considerable weight penalty. This can be achieved by adding stiffeners to the skin panel. Many studies are available on vibration analysis of isotropic panels. However, studies on the vibration and flutter analysis of stiffened anisotropic panels are rare.

In the present study, flutter analysis of a stiffened panel has been performed using the structural model[7] proposed by the present authors to study the vibrational characteristics of anisotropic plates with stiffeners that are stacked vertically with respect to the skin panel. This paper investigates the effects of the stiffener size and the fiber orientation on the flutter boundaries.

II. Governing Equation for Flutter Analysis

A first-order shear-deformable plate model for skin panel and a Timoshenko beam model for stiffeners are used in the finite element modeling of the stiffened anisotropic panel. The plate and beam finite elements have nine and three nodal points, respectively. The plate and beam elements are connected through the appropriate kinematic relations between the skin panel and stiffener.[7]

The aerodynamic pressure exerted on deflected panel at a supersonic speed can be obtained using linearized piston theory. The aerodynamic stiffness and damping matrices in flutter calculations can be derived using the virtual work done by the aerodynamic forces. The resulting finite element equations can be obtained for the entire system as follows[4–6]:

$$[M]\{\ddot{U}\} + g[A_d]\{\dot{U}\} + ([K] + \beta[A_f])\{U\} = \{0\} \tag{1}$$

where $[M]$, $[K]$, and $\{U\}$ are the mass and stiffness matrices and the displacement vector, respectively; $[A_d]$ and $[A_f]$ are the aerodynamic damping and stiffness matrices, respectively; and β and g are the aerodynamic pressure and damping parameter, respectively. Assuming $\{U\} = e^{\omega t}\{U\}$, and transforming Eq. (1) to the state-space form, one can get the following equation:

$$\left(\begin{bmatrix} [0] & [M] \\ [K] + \beta[A_f] & g[A_d] \end{bmatrix} - \omega \begin{bmatrix} [M] & [0] \\ [0] & -[M] \end{bmatrix} \right) \begin{Bmatrix} U \\ \dot{U} \end{Bmatrix} = \{0\} \tag{2}$$

Received Jan. 21, 1995; revision received Aug. 18, 1995; accepted for publication Nov. 14, 1995.

*Research Assistant, Department of Aerospace Engineering, 373-1, Kusong-Dong, Yusong-Gu.

†Associate Professor, Department of Aerospace Engineering, 373-1, Kusong-Dong, Yusong-Gu. Member AIAA.

When $\beta = 0$, the problem is reduced to that of the free vibration in vacuo. To save a tremendous amount of computational time in the flutter calculation when β is not zero, one can use the normal-mode method. The flutter boundaries can be obtained using an adequate number of normal modes. Generally, the system equation (2) involves complex eigenvalues, and we can write $\omega = \omega_r + i\omega_i$. The flutter boundary is determined by the condition that the real part of complex eigenvalue, ω_r, becomes positive and the amplitude of motion increases exponentially with time. For the simple representation, the useful nondimensional parameter[6] is introduced as $\beta^* = \beta a^3/D$, where $D = Ec^3/12(1 - \nu^2)$ for the isotropic case, and $D = E_2c^3$ for the anisotropic case; here ν is Poisson's ratio, a the side length of the panel, c the thickness of the panel, and E Young's modulus.

III. Results and Discussion

The model dimension and material properties are $a/b = 1.0$, $a/c = 150$, $h/c = 10.0$, $t/c = 2.0$, $E = 69$ GPa, $\rho = 2670$ kg/m^3, and $\nu = 0.3$. The boundary conditions of the panel are clamped at all edges. In the present analysis, 8 × 12 meshes and 25 modes have been selected because they guaranteed a good convergence of solutions from the convergence test.

First, we investigate how much a change of the material properties of the stiffener affects the flutter boundary. In this case, the material properties of the skin panel and the geometry of both skin panel and stiffener are unchanged. As the density and stiffness of the stiffener change gradually from lower to higher values, the flutter boundaries change as shown in Fig. 1. The stiffener mass attached to the center of the skin panel makes the critical dynamic pressure increase slightly. The stiffness of the stiffener greatly affects the flutter boundary, as shown in Fig. 1b. The flutter boundaries of the panels with a very soft stiffener and with a very stiff stiffener asymptotically approach those of the unstiffened panel and the unstiffened half panel, respectively. However, the flutter dynamic pressure for the stiffener with normal stiffness ($E = 69$ GPa) exceeds that of the unstiffened half panel for the following reason. The aeroelastic stability of the panel in a uniform airflow is governed by the relative spacing of its natural frequencies. The flutter occurs when two frequencies merge into one. Two in vacuo frequencies corresponding to the flutter mode in the unstiffened half panel are closer than in the panel with the stiffener of normal stiffness ($E = 69$ GPa). Hence, the flutter for the unstiffened half panel occurs at lower dynamic pressure than that for the normally stiffened panel.

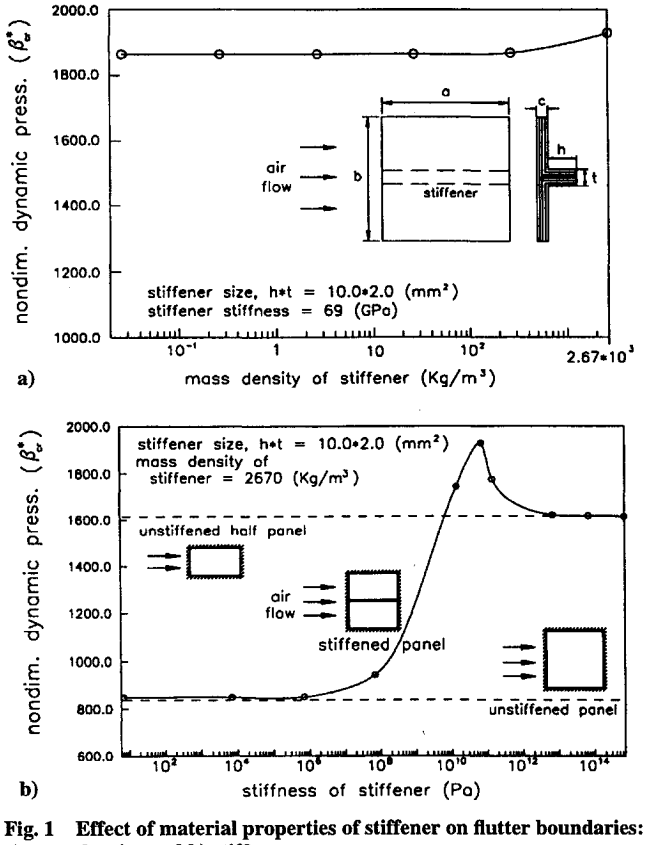

Fig. 1 Effect of material properties of stiffener on flutter boundaries: a) mass density and b) stiffness.

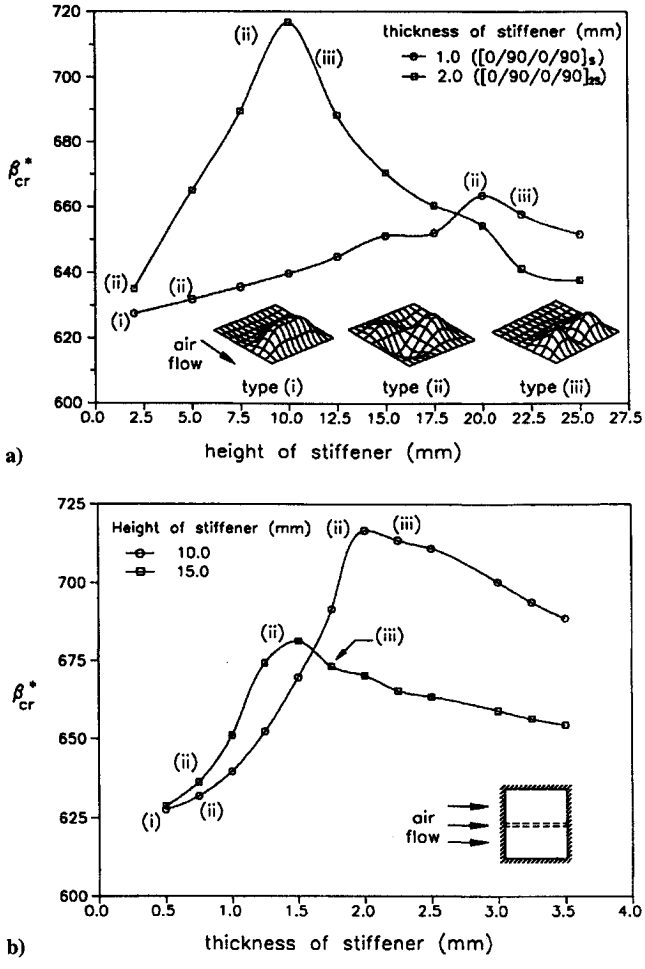

Fig. 2 Effect of stiffener size on flutter boundaries: a) effect of height change and b) effect of thickness change.

The effect of the stiffener size on the flutter boundary is next investigated. Stiffened anisotropic T300/5208 graphite–epoxy laminar plates are selected as examples. The material properties are given as $E_1 = 138$ GPa, $E_2 = 9.7$ GPa, $G_{12} = G_{13} = 5.5$ GPa, $G_{23} = 4.1$ GPa, $\nu_{12} = 0.3$, $\rho = 1580$ kg/m^3, and ply thickness = 0.125 mm. The geometry of the skin panel is the same as before ($a/c = 150$ and $c = 1.0$ mm), and only the stiffener size changes in this case. The boundary conditions are all clamped at every edge. The stacking sequence of the skin panel is $[0/90]_{2s}$, and that of the stiffener is [0/90/0/···/90/0]. The lamination scheme of the stiffener is that the 0- and 90-deg plies are alternately inserted in the middle surface of the stiffener, preserving the symmetric stacking sequence. Figure 2 shows the effect of the stiffener size on the flutter boundary of the stiffened square panel. The type of flutter mode changes according to the stiffener size of the stiffened panel. When the height of the stiffener is very small, the flutter mode is type (i) as shown in the inset of Fig. 2a. As the stiffener height increases, the flutter mode changes from type (i) to type (ii) and type (iii). In the flutter mode type (iii), the critical dynamic pressure decreases as the stiffener height increases. The optimal size of the stiffener is the value in which flutter mode type (ii) changes to the type (iii). Also, we can see that if the weight of the two stiffeners is nearly identical, the larger-thickness stiffener is better than the larger-height stiffener. The reason may be that flutter mode type (ii) is influenced by the rotary inertia of the stiffener, and the rotary inertia is influenced mainly by the height of the stiffener.

The effect of fiber orientation angle of the anisotropic stiffener on the flutter boundary is next investigated. The geometry of the

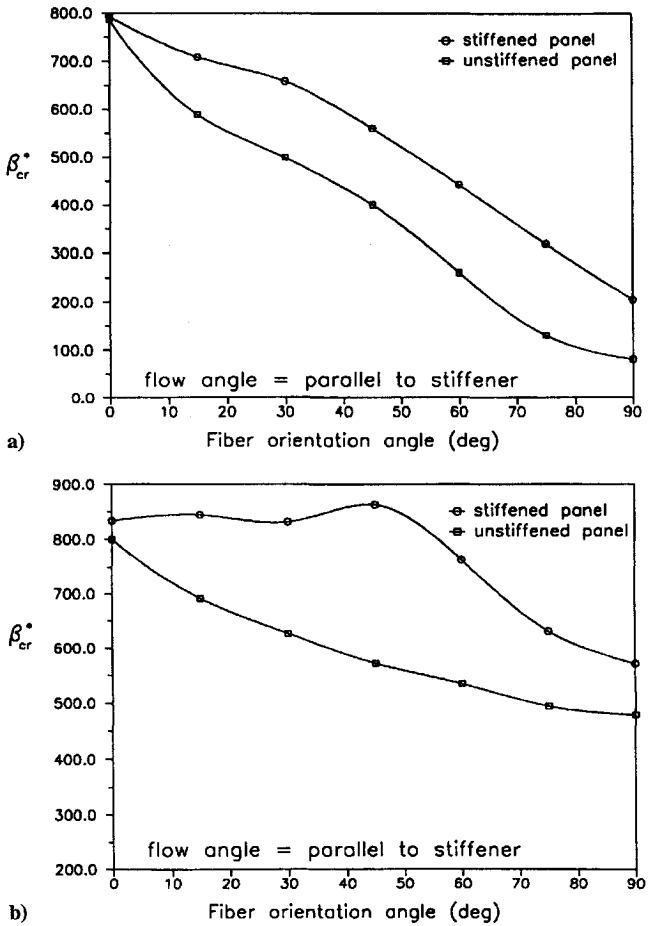

Fig. 3 Effect of stacking sequence on flutter boundaries: a) $[\pm\theta]_{2s}$ stiffened panel and b) $[0/\pm\theta/90]_s$ stiffened panel.

stiffened panel is $a/c = 200$, $t/c = 1.0$, and $h/c = 15$. The stacking sequence of the stiffener is identical with that of the skin panel. Two kinds of stiffened panels are selected as examples; the stacking sequence of the first panel is $[\pm\theta]_{2s}$, and that of the second is $[0/\pm\theta/90]_s$. Figure 3a shows that the critical dynamic pressure is greatly influenced by the fiber orientation. As the fiber orientation angle θ becomes perpendicular to the flow angle ϕ, the critical dynamic pressure of the first stiffened panel decreases monotonically. However, for the second panel, as shown in Fig. 3b, the critical dynamic pressure of the stiffened panel is nearly unchanged when the fiber orientation angle is less than 45 deg. The critical dynamic pressure of the stiffened panel becomes maximum near the fiber orientation angle of 45 deg. When the angle becomes larger than 45 deg, the critical dynamic pressure decreases monotonically. From this figure, one can conclude that the quasiisotropic lamination is a desirable stacking sequence for the flutter characteristics.

IV. Conclusion

A supersonic panel flutter analysis of a stiffened laminated panel has been carried out using linear piston theory with plate and beam finite elements based on a shear-deformable plate and a Timoshenko beam theory. Numerical results are obtained for the stiffened isotropic and anisotropic panels. This study is focused on the effects of the stiffener size and the fiber orientation angle on the flutter boundary. The following conclusions can be made.

There are three typical flutter modes according to the stiffener size in the stiffened panel. As the stiffener size increases, the type of the flutter mode changes from type (i) to type (ii), and from type (ii) to type (iii). The optimal size of the stiffener is the value where the flutter mode type (ii) changes to type (iii).

The present results show that the fiber orientation angle strongly influences the flutter boundary of the stiffened panel. The quasiisotropic lamination is a desirable stacking sequence from the viewpoint of flutter characteristics. This lamination scheme yields the maximum value for the critical dynamic pressure.

References

[1]Dowell, E. H., *Aeroelasticity of Plates and Shells*, Noordhoff International, Leyden, The Netherlands, 1975.

[2]Olson, M. D., "Some Flutter Solutions Using Finite Elements," *AIAA Journal*, Vol. 8, No. 4, 1970, pp. 747–752.

[3]Bismarck-Nasr, M. N., "Finite Element Analysis of Aeroelasticity of Plates and Shells," *ASME Applied Mechanics Review*, Vol. 45, No. 12, 1992, pp. 461–482.

[4]Lee, I., and Cho, M. H., "Supersonic Flutter Analysis of Clamped Symmetric Composite Panels Using Shear Deformable Finite Elements," *AIAA Journal*, Vol. 29, No. 5, 1991, pp. 782, 783.

[5]Liaw, D. G., "Supersonic Flutter of Laminated Thin Plates with Thermal Effects," *Journal of Aircraft*, Vol. 30, No. 1, 1993, pp. 105–111.

[6]Pidaparti, R. M. V., and Yang, T. Y., "Supersonic Flutter Analysis of Composite Plates and Shells," *AIAA Journal*, Vol. 31, No. 6, 1993, pp. 1109–1117.

[7]Lee, D. M., and Lee, I., "Vibration Analysis of Anisotropic Plates with Eccentric Stiffener," *Computers and Structures*, Vol. 57, No. 1, 1995, pp. 99–105.